J|A|C|S
ARTICLES
Published on Web 11/12/2003

Hemilabile Ligands in Organolithium Chemistry: Substituent Effects on Lithium Ion Chelation

Antonio Ramírez, Emil Lobkovsky, and David B. Collum*

Contribution from the Department of Chemistry and Chemical Biology, Baker Laboratory, Cornell University, Ithaca, New York 14853-1301

Received May 28, 2003; E-mail: dbc6@cornell.edu

Abstract: The lithium diisopropylamide-mediated 1,2-elimination of 1-bromocyclooctene to provide cyclooctyne is investigated using approximately 50 potentially hemilabile polyethers and amino ethers. Rate laws for selected ligands reveal chelated monomer-based pathways. The dependence of the rates on ligand structure shows that anticipated rate accelerations based on the *gem*-dimethyl effect are nonexistent and that substituents generally retard the reaction. With the aid of semiempirical and DFT computational studies, the factors influencing chelation are discussed. It seems that severe buttressing within chelates of the substitutionally rich ligands precludes a net stabilization of the chelates relative to nonchelated (η^1-solvated) forms. One ligand—$MeOCH_2CH_2NMe_2$—appears to promote elimination uniquely by a higher-coordinate monomer-based pathway.

Introduction

We have been exploring the role of hemilabile ligands in organolithium chemistry (Scheme 1).[1] Although most applications of hemilabile ligands exploit observable chelates that readily liberate a coordination site,[2] we take a slightly different approach. By using a ligand that is η^1-coordinated in the reactant and η^2-coordinated at the rate-limiting transition structure, we achieve two goals. First, restricting chelation to the transition structure(s) maximizes the benefits of chelation by eliminating counterproductive stabilization of the reactant. Previous investigations have revealed lithium diisopropylamide (LDA)-mediated reactions can be accelerated up to 10000-fold by hemilabile ligands due to the intervention of monomer- or dimer-based pathways (Scheme 1). Second, the absence of chelation in the ground state allows one to assess how a pendant coordinating moiety (L), chain length, and other structural features within the ligand (S) influence chelation at the transition state. It is this probative value of hemilabile ligands that most piques our interest.[3−5]

In this contribution we exploit the LDA-mediated dehydrohalogenation of 1-bromocyclooctene[6,7] (eq 1), attempting to ask a simple question: Is there a *gem*-dimethyl effect on lithium ion chelation? The *gem*-dimethyl effect results when destabilizing interactions caused by substitution in an acyclic form—*geminal* dimethylation, for example—are alleviated by ring closure (eq 2).[8−11] The cyclic transition structures often lead to newly formed carbocyclic or heterocyclic rings[12] but can be fleeting cyclic transition structures en route to acyclic products.[13] The substituent-dependent accelerations can be pronounced (up to 10^4).[14] The role of substitution on lithium chelates has not been studied in detail.[9] For this specific case study, an extensive survey of a number of hemilabile ligands and assorted potentially hemilabile polyfunctional ligands (Charts 1−3) reveals little evidence of the *gem*-dimethyl effect. We were forced, therefore,

(1) (a) Remenar, J. F.; Collum, D. B. *J. Am. Chem. Soc.* **1997**, *119*, 5573. (b) Ramírez, A.; Collum, D. B. *J. Am. Chem. Soc.* **1999**, *121*, 11114. (c) Remenar, J. F.; Collum, D. B. *J. Am. Chem. Soc.* **1998**, *120*, 4081.

(2) For reviews of hemilabile ligands, see: Braunstein, P.; Naud, F. *Angew. Chem., Int. Ed.* **2001**, *40*, 680. Slone, C. S.; Weinberger, D. A.; Mirkin, C. A. *Progr. Inorg. Chem.* **1999**, *48*, 233. Lindner, E.; Pautz, S.; Haustein, M. *Coord. Chem. Rev.* **1996**, *155*, 145. Bader, A.; Lindner, E. *Coord. Chem. Rev.* **1991**, *108*, 27. For recent references of hemilabile ligands, see: Kuriyama, M.; Nagai, K.; Yamada, K. I.; Miwa, Y.; Taga, T.; Tomioka, K. *J. Am. Chem. Soc.* **2002**, *124*, 8932. Park, H.; RajanBabu, T. V. *J. Am. Chem. Soc.* **2002**, *124*, 734. Romeo, R.; Monsu' Scolaro, L.; Plutino, M. R.; Romeo, A.; Nicolo', F.; Del Zotto, A. *Eur. J. Inorg. Chem.* **2002**, *3*, 629. Liu, X.; Stern, C. L.; Mirkin, C. A. *Organometallics* **2002**, *21*, 1017. Rogers, C. W.; Wolf, M. O. *Angew. Chem., Int. Ed.* **2002**, *41*, 1898. Braunstein, P.; Naud, F.; Dedieu, A.; Rohmer, M.-M.; DeCian, A.; Rettig, S. J.; *Organometallics* **2001**, *20*, 2966. Roch-Neirey, C.; Le Bris, N.; Clément, J.-C.; des Abbayes, H. *Tetrahedron Lett.* **2001**, *42*, 643. Faller, J. W.; Stokes-Huby, H. L.; Albrizzio, M. A. *Helv. Chim. Acta* **2001**, *84*, 3031. Deckers, P. J. W.; Hessen, B.; Teuben, J. H. *Angew. Chem., Int. Ed.* **2001**, *40*, 2516.

(3) (a) Reich, H. J.; Goldenberg, W. S.; Sanders, A. W.; Jantzi, K. L.; Tzschucke, C. C. *J. Am. Chem. Soc.* **2003**, *125*, 3509 and references therein. (b) Snieckus, V. *Chem. Rev.* **1990**, *90*, 879. (c) Klumpp, G. W. *Recl. Trav. Chim. Pays-Bas* **1986**, *105*, 1.

(4) Collum, D. B. *Acc. Chem. Res.* **1992**, *25*, 448.

(5) For related applications of hemilabile amino alkoxides of aluminum, see: Francis, J. A.; McMahon, N.; Bott, S. G.; Barron, A. R. *Organometallics* **1999**, *18*, 4399.

(6) Brandsma, L.; Verkruijsse, H. D. *Synthesis* **1978**, 290.

(7) For leading references to base-mediated eliminations of vinyl halides, see: Jacobs, T. L. *Org. React.* **1949**, *5*, 1. Bohlmann, F. *Angew. Chem.* **1957**, *69*, 82. Franke, G.; Ziengenbein, W.; Meister, H. *Angew. Chem.* **1960**, *72*, 391. Arens, J. F. In *Advances in Organic Chemistry*; Interscience Publishers: New York, 1960; Vol 2, p 121. Kobrich, G. *Angew. Chem., Int. Ed. Engl.* **1965**, *4*, 49. Kobrich, G.; Buck, P. In *Chemistry of Acetylenes*; Viehe, H. G., Ed.; Marcel Dekker: New York, 1969; p 99. Brandsma, L. In *Preparative Acetylenic Chemistry*; Elsevier: Amsterdam, 1971. Nakagawa, M. In *The Chemistry of the Carbon−Carbon Triple Bond;* Patai, S., Ed.; Wiley: Chichester, 1978; p 635. Ben-Efraim, D. A. In *The Chemistry of the Carbon−Carbon Triple Bond;* Patai, S., Ed.; Wiley: New York, 1978; p 755. Demlow, E. V.; Lisse, M. *Liebigs Ann. Chem.* **1980**, 1. Brandsma, L.; Verkruijsse, H. D. *Synthesis of Acetylenes, Allenes and Cumulenes*; Elsevier: Amsterdam, 1988. Gleiter, R.; Merger, R. In *Modern Acetylene Chemistry;* Stang, P. J.; Diederich, F., Ed.; VCH: Weinheim, 1995; p 285. Furber, M. In *Comprehensive Organic Functional Group Transformations*; Katrizky, A. R., Meth-Cohn, O., Rees. C. W., Eds.; Pergamon: Oxford, 1995; Vol. 1, p 1062.

10.1021/ja030322d CCC: $25.00

Scheme 1

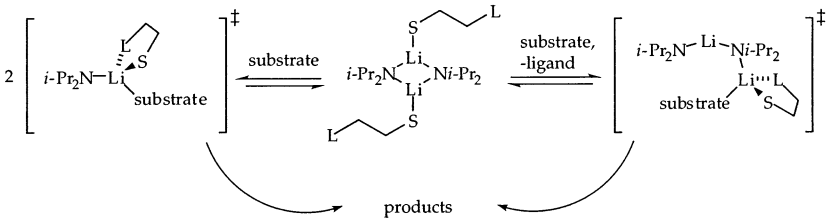

Chart 1. Relative Rate Constants (in parentheses) for the Dehydrobromination of **1** by LDA Solvated by Unsubstituted Ethanolamine-derived Amino Ethers

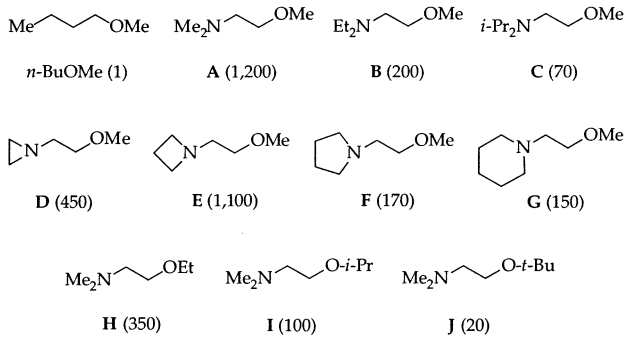

to rephrase the original question: *Why* is there no *gem*-dimethyl effect? This question leads us to consider the dominant and complex steric effects that influence metal ion chelation. As part of this study we revisit the long-standing problem of choosing the appropriate reference state when studying the chelate effect.[15,16]

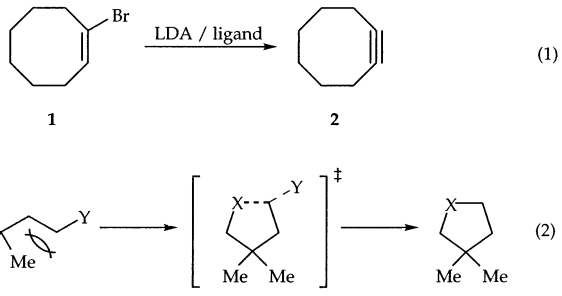

(1)

(2)

Results

The results are presented sequentially as follows: (1) Rate studies establish the dominance of monomer-based eliminations; (2) semiempirical (MNDO) computational studies address how ligand structure influences the stabilities of chelates relative to their open (η^1) forms; (3) DFT methods probe nuances of the LDA-mediated *syn*-elimination, including an elimination pathway via a highly solvated LDA monomer.

General Methods. LDA was prepared as a white crystalline solid.[17] The ligands in Charts 1−3 are commercially available, reported in the literature,[18] or readily available from modified syntheses (Supporting Information). ^{6}Li and ^{15}N NMR spectroscopic studies[19,20] show [^{6}Li,^{15}N]LDA[17] to be solvated by a number of amino ethers and related polyfunctional ligands to be η^1-solvated dimers. The distinction of *O*- rather than *N*-bound coordination is consistent with previous studies showing that ethers are superior to sterically demanding trialkylamines as

(8) Kirby, A. *J. Adv. Phys. Org. Chem.* **1980**, *17*, 183. Hammond, G. S. *Steric Effects in Organic Chemistry*, Newman, M. S. Ed., Wiley: New York, 1956. Eliel, E. *Stereochemistry of Carbon Compounds*; McGraw-Hill Book Comp.: New York, 1962; p 197. Capon, B.; McManus, S. P. *Neighboring Group Participation*; Plenum Press: New York, 1976; Vol. I, p 43. See also: Galli, C.; Mandolini, L. *Eur. J. Org. Chem.* **2000**, 3117. Jung, M. E. *Synlett* **1999**, 843. Parrill, A. L.; Dolata, D. P. *J. Mol. Struct.* (THEOCHEM) **1996**, *370*, 182. Lightstone, F. C.; Bruice, T. C. *J. Am. Chem. Soc.* **1994**, *116*, 10789. Parrill, A. L.; Dolata, D. P. *Tetrahedron Lett.* **1994**, *35*, 7319. Keese, R.; Meyer, M. *Tetrahedron* **1993**, *49*, 2055. Jung, M. E.; Gervay, J. *J. Am. Chem. Soc.* **1991**, *113*, 224. Schleyer, P. v. R. *J. Am. Chem. Soc.* **1961**, *83*, 1368. Allinger, N. L.; Zalkow, V. *J. Org. Chem.* **1960**, *25*, 701. Bruice, T. C.; Pandit, U. K. *J. Am. Chem. Soc.* **1960**, *82*, 5858.

(9) The *gem*-dimethyl effect and affiliated Thorpe−Ingold effect[10] have been discussed in the context of organometallic chemistry: Bessel, C. A.; Aggarwal, P.; Marschilok, A. C.; Takeuchi, K. J. *Chem. Rev.* **2001**, *101*, 1031. Casey, C. P.; Klein, J. F.; Fagan, M. A. *J. Am. Chem. Soc.* **2000**, *122*, 4320. Faller, J. W.; Patel, B. P.; Albrizzio, M. A.; Curtis, M. *Organometallics* **1999**, *18*, 3096. Barkley, J.; Ellis, M.; Higgins, S. J.; McCart, M. K. *Organometallics* **1998**, *17*, 1725. Desper, J. M.; Gellman, S. H.; Wolf, R. E., Jr.; Cooper, S. R. *J. Am. Chem. Soc.* **1991**, *113*, 8663. Uemura, M.; Minami, T.; Hayashi, Y. *J. Am. Chem. Soc.* **1987**, *109*, 5278. Shaw, B. L. *J. Organomet. Chem.* **1980**, *200*, 307. Shaw, B. L.; Weeks, B. *J. Chem. Soc., Dalton Trans.* **1979**, 1972. Shaw, B. L. *J. Am. Chem. Soc.* **1975**, *97*, 3856. Al-Salem, N. A.; Empsall, H. D.; Markham, R.; Newman, M. S.; Busch, D. H.; Cheney, G. E.; Gustafson, C. R. *Inorg. Chem.* **1972**, *12*, 2890.

(10) Beesley, R. M.; Ingold, C. K.; Thorpe, J. F. *J. Chem. Soc.* **1915**, *107*, 1080. Ingold, C. K. *J. Chem. Soc.* **1921**, *119*, 305.

(11) Also, see the rigid group principle: Schmiegel, J.; Funke, U.; Mix, A.; Gruetzmacher, H. F. *Chem. Ber.* **1990**, *123*, 1397. Voegtle, F.; Mayenfels, P.; Luppertz, F. *Synthesis* **1984**, 580. Rasshofer, W.; Oepen, G.; Mueller, W. M.; Voegtle, F. *Chem. Ber.* **1978**, *111*, 1108. Siemeing, U. *Polyhedron* **1997**, *16*, 1513.

(12) Yamamoto, Y.; Takagishi, H.; Itoh, K. *J. Am. Chem. Soc.* **2002**, *124*, 28. Hicks, F. A.; Buchwald, S. L.; *J. Am. Chem. Soc.* **1996**, *118*, 11688. Jung, M. E.; Trifunovich, I. D.; Lensen, N. *Tetrahedron Lett.* **1992**, *33*, 6719. Hill, E. A.; Link, D. C.; Donndelinger, P. *J. Org. Chem.* **1981**, *46*, 1177. Eliel, E. L.; Knox, D. E. *J. Am. Chem. Soc.* **1985**, *107*, 2946. McIntyre, S.; Sansbury, F. H.; Warren, S. *Inorg. Chim. Acta* **1984**, *89*, 157.

(13) Tüzün, N. S.; Aviyente, V.; Houk, K. N. *J. Org. Chem.* **2002**, *67*, 5068. Kende, A. S.; Journet, M. *Tetrahedron Lett.* **1995**, *36*, 3087.

(14) Brown, R. F.; van Gulick, N. M. *J. Org. Chem.* **1956**, *21*, 1046.

(15) (a) Frausto da Silva, J. J. R. *J. Chem. Educ.* **1983**, *60*, 390. (b) Simmons, E. L. *J. Chem. Educ.* **1979**, *56*, 578. (c) Rosseinsky, D. R. *J. Chem. Soc., Dalton Trans.* **1979**, 731. (d) Munro, D. *Chem. Br.* **1977**, *13*, 100. (e) Hancock, R. D.; Marsicano, F. *J. Chem. Soc., Dalton Trans.* **1976**, 1096. (f) Jones, G. R. H.; Harrop, R. *J. Inorg. Nucl. Chem.* **1973**, *35*, 173. (g) Manhas, B. S. *Res. J. Sci.* **1974**, *1*, 16. (h) Bent, H. A. *J. Phys. Chem.* **1956**, *60*, 123.

(16) Rutherford, J. L.; Hoffmann, D.; Collum, D. B. *J. Am. Chem. Soc.* **2002**, *124*, 264.

(17) Kim, Y.-J.; Bernstein, M. P.; Galiano-Roth, A. S.; Romesberg, F. E.; Fuller, D. J.; Harrison, A. T.; Collum, D. B.; Williard, P. G. *J. Org. Chem.* **1991**, *56*, 4435.

(18) (a) **A**, **B**, **F**, **G**: Remenar, J. F.; Lucht, B. L.; Collum, D. B. *J. Am. Chem. Soc.* **1997**, *119*, 5567. (b) **C**: Brown, H. C.; Zaidlewicz, M.; Dalvi, P. V.; Narasimhan, S.; Mukhopadyay, A. *Organometallics* **1999**, *18*, 1305. (c) **D**: Buøen, S.; Dale, J. *Acta Chem. Scand.* **1986**, *B40*, 278. (d) **E**: Sammes, P. G.; Smith, S. *J. Chem. Soc., Perkin Trans. 1* **1984**, 2415; see also ref 1a. (e) **H**: Haarstad, V. B.; Domer, F. R.; Chihal, D. M.; Rege, A. B.; Charles, H. C. *J. Med. Chem.* **1976**, *19*, 760. (f) **I**, **J**: Eckhardt, G. *Org. Mass. Spectrom.* **1979**, *14*, 31. (g) **L**, **M**: Cope, A. C.; Kliegman, J. M.; Friedrich, E. C. *J. Am. Chem. Soc.* **1967**, *89*, 287. (h) **P**: Seebach, D.; Kalinowski, H.-O.; Bastani, B.; Crass, G.; Daum, H.; Dörr, H.; DuPreez, V. E.; Langer, W.; Nüssler, C.; Dei, H.-A.; Schmidt, M. *Helv. Chim. Acta* **1977**, *60*, 301. (i) **S**, **T**: Di Vona, M. L.; Illuminati, G.; Lillocci, C. *J. Chem. Soc., Perkin Trans 2* **1985**, 1943. (j) **U**, **V**: Coote, S. J.; Davis, S. G.; Goodfellow, C. L.; Sutton, K. H.; Middlemiss, D.; Naylor, A. *Tetrahedron: Asymmetry* **1990**, *1*, 817. (k) **W**: Pine, S. H.; Sánchez, B. L. *J. Org. Chem.* **1971**, *36*, 829. (l) **X**: Traynelis, V. J.; Dadura, J. G. *J. Org. Chem.* **1961**, *26*, 686. (m) **Y**: Seebach, D.; Kalinowski, H.-O.; Bastani, B.; Crass, G.; Daum, H.; Dörr, H.; DuPreez, V. E.; Langer, W.; Nüssler, C.; Oei, H.-A.; Schmidt, M. *Helv. Chim. Acta* **1977**, *60*, 301. (n) **Z**: Shultz, O. E.; Ziegler, A. *Pharmazie* **1970**, *25*, 472. (o) **AA**: Periasamy, M.; Ramanathan, C. R.; Kumar, N. S. *Tetrahedron: Asymmetry* **1999**, *10*, 2307.

Chart 2. Relative Rate Constants (in parentheses) for the Dehydrobromination of **1** by LDA Solvated by Mono- and Disubstituted Ethanolamine-derived Amino Ethers

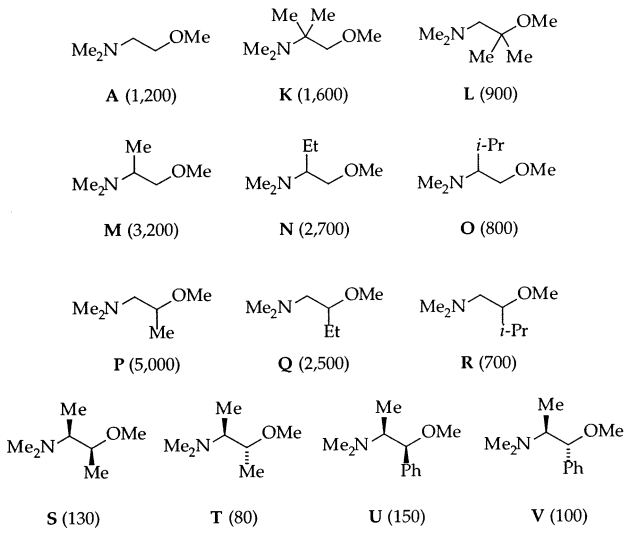

ligands for hindered lithium amide dimers.[1,21,22] Spectral data for a number of solvated dimers (**3**) not previously characterized are included in Supporting Information.

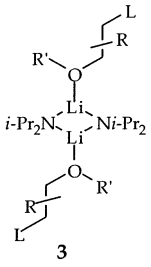

3

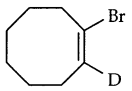

1-d_1

LDA/*n*-BuOMe. Rate studies of the LDA/*n*-BuOMe-mediated dehydrohalogenation of **1** (eq 1) provide a foundation for understanding hemilabile ligands and for illustrating general experimental protocols. Pseudo-first-order conditions were established by maintaining the concentration of 1-bromocyclooctene (**1**) at 0.004 M. LDA, and *n*-BuOMe concentrations were maintained high, yet adjustable, using hexane as the cosolvent.[23] Loss of **1** monitored by gas chromatography relative to an internal decane standard follows clean first-order behavior. The resulting pseudo-first-order rate constants (k_{obsd}) are independent of the initial concentration of **1**, confirming first-order dependence.[24] A significant isotope effect (k_H/k_D) determined by comparing the independently measured rate constants for the elimination of **1** and **1-d_1**[25] (Table 1) confirms a rate-limiting proton transfer. Plots of k_{obsd} versus [LDA] and k_{obsd} versus [*n*-BuOMe] (Figures 1 and 2) reveal half-order and zeroth-order dependencies, respectively. The reaction orders and the kinetic isotope effect (Table 1, entry 1) are consistent with the idealized rate law in eq 4, the mechanism described

Table 1. Summary of Rate Studies for the LDA-Mediated β-elimination of **1** (eq 1)

		LDA[a] ligand			
entry	T, °C	ligand	order	order	k_H/k_D
1	0	*n*-BuOMe	0.51 ± 0.02	0	2.1 ± 0.2
2	−40	**A**	0.52 ± 0.03	0.93 ± 0.07	3.0 ± 0.2
3	−40	**A**	0.49 ± 0.03[b]	−	4.6 ± 0.5
4	−40	**B**	0.45 ± 0.04	0	2.4 ± 0.3
5	−40	**H**	0.50 ± 0.03	0	2.6 ± 0.3
6	−40	**CC**	0.51 ± 0.01	0	2.5 ± 0.3
7	−40	**DD**	0.49 ± 0.03	0	2.2 ± 0.2

[a] [Ligand] = 0.5 M. [b] [Ligand] = 6.0 M.

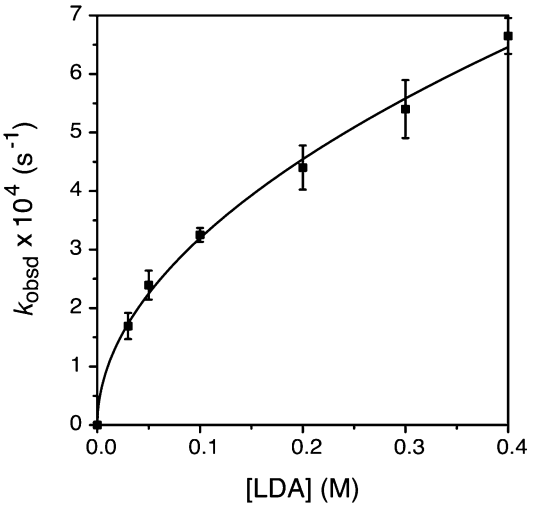

Figure 1. Plot of k_{obsd} vs [LDA] in *n*-BuOMe (0.5 M) and hexane cosolvent for the β-elimination of 1-bromocyclooctene (**1**, 0.004 M) at 0 °C. The curve depicts the result of an unweighted least-squares fit to $k_{obsd} = k[\text{LDA}]^n$ ($k = 1.0 \pm 0.1 \times 10^{-5}$, $n = 0.51 \pm 0.02$).

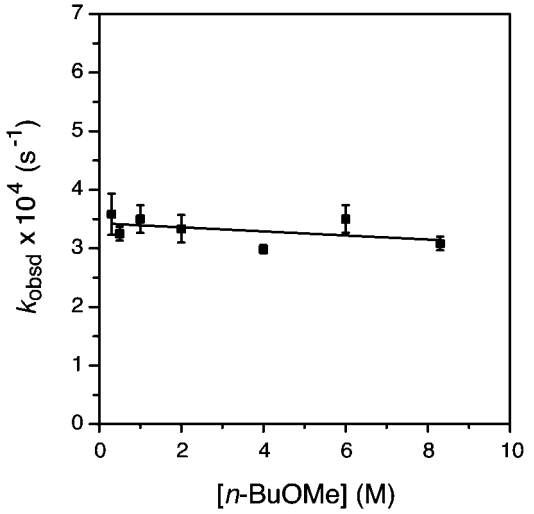

Figure 2. Plot of k_{obsd} vs [*n*-BuOMe] in hexane cosolvent for the β-elimination of 1-bromocyclooctene (**1**, 0.004 M) by LDA (0.10 M) at 0 °C. The curve depicts the result of an unweighted least-squares fit to $k_{obsd} = k[n\text{-BuOMe}] + k'$ ($k = -3 \pm 3 \times 10^{-8}$, $k' = 3.4 \pm 0.1 \times 10^{-6}$).

(19) Collum, D. B. *Acc. Chem. Res.* **1993**, *26*, 227. For other reviews of structural investigations of lithium amides, see: Gregory, K.; Schleyer, P. v. R.; Snaith, R. *Adv. Inorg. Chem.* **1991**, *37*, 47. Mulvey, R. E. *Chem. Soc. Rev.* **1991**, *20*, 167. Beswick, M. A.; Wright, D. S. In *Comprehensive Organometallic Chemistry II*; Abels, F. W., Stone, F. G. A., Wilkinson, G., Eds.; Pergamon: New York, 1994; Vol. 1, Chapter 1. Lucht, B. L.; Collum, D. B. *Acc. Chem. Res.* **1999**, *32*, 1035.

(20) Spectroscopic studies of [^{6}Li,^{15}N]LDA solvated ligands **H**-**R** are archived in Supporting Information.

(21) (a) Bernstein, M. P.; Collum, D. B. *J. Am. Chem. Soc.* **1993**, *115*, 8008. (b) Lucht, B. L.; Collum, D. B. *J. Am. Chem. Soc.* **1996**, *118*, 2217. (c) Also, see ref 1a.

(22) For a crystal structure of an LiHMDS−LiCl mixed aggregate containing $MeOCH_2CH_2NMe_2$ (**A**), see: Henderson, K. W.; Dorigo, A. E.; Liu, Q.-Y.; Williard, P. G.; Schleyer, P. v. R.; Bernstein, P. R. *J. Am. Chem. Soc.* **1996**, *118*, 1339.

(23) The concentration of the lithium amide, although expressed in units of molarity, refers to the concentration of the monomer unit (normality).

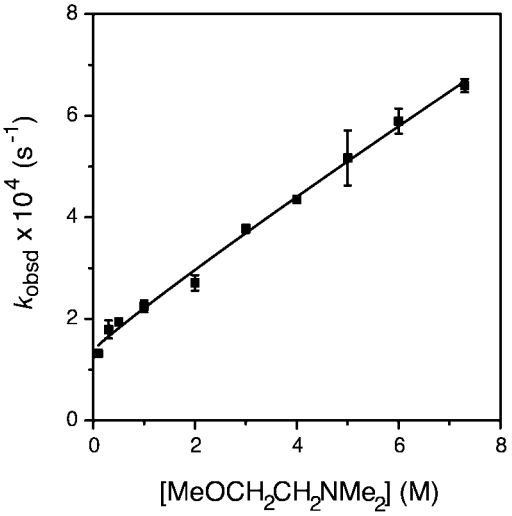

Figure 3. Plot of k_{obsd} vs [$MeOCH_2CH_2NMe_2$] in hexane cosolvent for the β-elimination of 1-bromocyclooctene (**1**, 0.004 M) by LDA (0.10 M) at −40 °C. The curve depicts the result of an unweighted least-squares fit to $k_{obsd} = k[MeOCH_2CH_2NMe_2]^n + k'$ ($k = 8 \pm 1 \times 10^{-5}$, $k' = 1.4 \pm 0.1 \times 10^{-4}$, $n = 0.93 \pm 0.07$).

generically in eqs 5 and 6, and a monomer-based transition structure such as **4**.

$$-\mathrm{d}[\mathbf{1}]/\mathrm{d}t = k'[\mathbf{1}]^1[\mathrm{LDA}]^{1/2}[n\text{-BuOMe}]^0 \quad (4)$$

$$^1/_2(i\text{-Pr}_2\text{NLi})_2(n\text{-BuOMe})_2 \rightleftharpoons (i\text{-Pr}_2\text{NLi})(n\text{-BuOMe}) \quad (5)$$

$$(i\text{-Pr}_2\text{NLi})(n\text{-BuOMe}) + \mathbf{1} \rightarrow [(i\text{-Pr}_2\text{NLi})(n\text{-BuOMe})(\mathbf{1})]^{\ddagger} \quad (6)$$

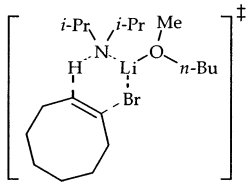

4

LDA/$ROCH_2CH_2NR'_2$. Rate studies using LDA/**A** mixtures carried out as described above afforded unexpected results. A plot of k_{obsd} versus [**A**] (Figure 3) displays linear dependence and a substantial nonzero intercept. The nonzero intercept is emblematic of a ligand-concentration-independent pathway similar to that noted in other LDA/[**A**]-mediated dehydrohalogenations.[1c] The previously undetected concentration dependence could be attributed to either (1) a second pathway requiring an associative solvation of lithium, or (2) an unusually large[26] generalized medium effect. To distinguish these two possibilities we investigated the kinetics using closely related amino ethers **B** and **H**, which contained slightly larger coordinating functionalities. Plots of k_{obsd} versus [**B**] and k_{obsd} versus [**H**] show no concentration dependencies whatsoever (Table 1, entries 4 and 5). Therefore, we attribute the linear dependence in Figure 3 to a sterically sensitive (primary shell) solvation event that can only occur when *both* coordinating functionalities on the difunctional ligand are small.

Plots of k_{obsd} versus [LDA] reveal half-order LDA dependencies at both low and high concentrations of ligand **A**. The idealized rate law (eq 7) is consistent with two monomer-based pathways with transition structures $[(i\text{-Pr}_2\text{NLi})(\mathbf{A})(\mathbf{1})]^{\ddagger}$ (eqs 5 and 6) and $[(i\text{-Pr}_2\text{NLi})(\mathbf{A})_2(\mathbf{1})]^{\ddagger}$ (eqs 8 and 9). The ligand-concentration-independent pathway is discussed in the context of a chelated transition structure **5**. The ligand-concentration-dependent pathway (eqs 8 and 9) forces us to consider a range of isomeric transition structures (**6**−**10**). All have been explored computationally as described below.

$$-\mathrm{d}[\mathbf{1}]/\mathrm{d}t = k'[\mathbf{1}][\mathrm{LDA}]^{1/2}[\mathbf{A}]^0 + k'[\mathbf{1}][\mathrm{LDA}]^{1/2}[\mathbf{A}] \quad (7)$$

$$\mathbf{A} + {}^1/_2(i\text{-Pr}_2\text{NLi})_2(\mathbf{A})_2 \rightleftharpoons (i\text{-Pr}_2\text{NLi})(\mathbf{A})_2 \quad (8)$$

$$(i\text{-Pr}_2\text{NLi})(\mathbf{A})_2 + \mathbf{1} \rightarrow [(i\text{-Pr}_2\text{NLi})(\mathbf{A})_2(\mathbf{1})]^{\ddagger} \quad (9)$$

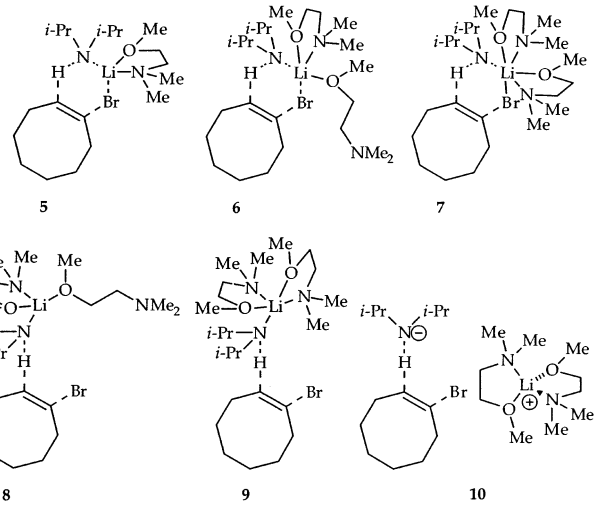

5 **6** **7**

8 **9** **10**

LDA/$MeOCH_2CH_2OR$. Rate laws for the LDA-mediated elimination of **1** in the presence of dimethoxyethane (DME, **CC**; see Table 1, entry 6) and *tert*-butoxymethoxyethane (*t*-$BuOCH_2CH_2OMe$, **DD**; see Table 1, entry 7) were completed as described above. The rate laws, in conjunction with the rate accelerations, are consistent with eliminations via exclusively chelated monomers (eqs 5 and 6) analogous to **5**. It is notable that, despite its relatively low steric demands compared to amino ether **A**, DME does *not* facilitate the elimination via a more highly solvated form.

Solvent-Dependent Relative Rates. The relative rate constants for the LDA-mediated elimination are summarized in Charts 1−3. Although detailed rate studies were not carried out in most cases, cross-checks showing ligand-concentration-independent rates for a number of ligands implicate a mechanistic homogeneity. Inspection of the relative rates reveals that substitution on the ligand backbones can either accelerate or decelerate the elimination; ligands **M** and **P**, bearing a single methyl, provide the largest (albeit modest) rate acceleration when compared to the unsubstituted amino ether **A**. The ligands in Chart 3 were the most randomly chosen. If a pronounced

(24) Espenson, J. H. *Chemical Kinetics and Reaction Mechanisms*; McGraw-Hill: New York, 1995; p 15.
(25) 1-Bromocyclooctene-2-*d* (**1**-d_1) was prepared following the procedure reported in ref 6 starting from (*Z*)-cyclooctene-1, 2-d_2: Hayward, R. C.; Whitham, G. H. *J. Chem. Soc., Perkin Trans. 1* **1975**, 2267.
(26) Aubrecht, K. B.; Winemiller, M. D.; Collum, D. B. *J. Am. Chem. Soc.* **2000**, *122*, 11084. Galiano-Roth, A. S.; Collum, D. B. *J. Am. Chem. Soc.* **1989**, *111*, 6772. See ref 21a.

Chart 3. Relative Rate Constants (in parentheses) for the Dehydrobromination of **1** by LDA Solvated by Assorted Polyfunctional Ligands

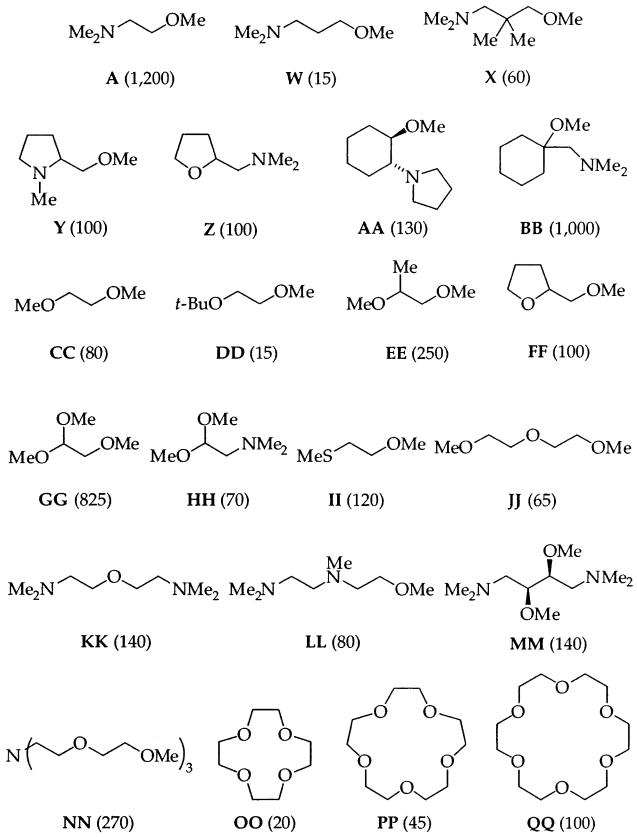

acceleration had appeared, additional structural and mechanistic studies would have followed, but no large accelerations were forthcoming.[27]

MNDO Computational Studies. We used MNDO computational methods to investigate how substitutions on the amino and alkoxy moieties, the carbon backbone of the ligand, and the lithium amide fragment influence the stabilities of chelates relative to their open-chain counterparts.[28] The transition structures for the eliminations were too congested to obtain useful results from MNDO;[29] therefore, the factors influencing chelation and the affiliated *gem*-dimethyl effect were investigated by studying the ligand-dependent dimer−monomer equilibria (Scheme 2). Although H_2NLi, Me_2NLi, and *i*-Pr_2NLi were used as models, distortions resulting from steric congestion were acute for the *i*-Pr_2NLi (LDA) fragment. Moreover, H_2NLi−

Scheme 2

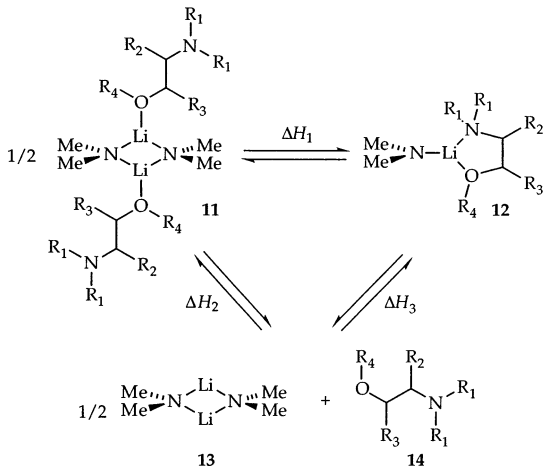

Table 2. Calculated Enthalpies (kcal/mol) of Monomer Aggregation (ΔH_1), Dimer Solvation (ΔH_2), and Monomer Solvation (ΔH_3) for Me_2NLi Coordinated to Ligands of General Structure $MeOCH_2CH_2NR_2$[a]

ligand	$H_{f(Ligand)}$	ΔH_1	ΔH_2	ΔH_3
A	−44.1	10.4	−6.8	3.6
B	−51.0	11.3	−7.1	4.2
C	−50.3	16.0	−6.2	9.8
D	−17.9	9.0	−6.7	2.3
E	−37.9	10.0	−6.8	3.2
F	−54.6	12.4	−6.8	5.6
G	−55.9	13.6	−6.8	6.8
av dev[b]	−	2.4	0.3	2.6

[a] The heats of formation (kcal/mol) of ligands **A**−**G** in their most stable conformations are represented by $\Delta H_{f(Ligand)}$. $(Me_2NLi)_2 = -60.5$ kcal/mol. [b] Av dev = average deviation.

ligand combinations often manifested seemingly spurious interactions between the lithiums and carbons within the ligand backbone. As noted previously,[28a] Me_2NLi appears to be the best computational model of LDA. Selected results for Me_2NLi are summarized in Scheme 2, Tables 2 and 3, and Figures 4−10. The enthalpies are quoted on a per-lithium basis. The *x* and *y* axes on the figures were intentionally fixed to a constant range of kcal/mol to avoid misleading visual distortions. Additional data for Me_2NLi as well as the data for both H_2NLi and *i*-Pr_2NLi are archived in Supporting Information.[30]

We explored the principle of hemilability in its simplest form by focusing on the ligands of general structure $MeOCH_2CH_2NR_2$ (Table 2). The mode of action of hemilabile ligands is foreshadowed by the average deviations (av dev) listed as the final entry in Table 2. The enthalpy of aggregation (ΔH_1) and solvation of the monomer (ΔH_3) manifest large average deviations indicative of strong ligand dependencies. In contrast, the small average deviation for the solvation of the dimer (ΔH_2) is consistent with ligand independence. Indeed, plots of ΔH_1 versus ΔH_2 and ΔH_1 versus ΔH_3 (Figures 4 and 5) show that the

(27) The failure of the crown ethers (**OO**-**QQ**, Chart 3) to promote rate accelerations that exceed those of simple diethers (**CC** and **JJ**) is consistent with structural studies showing crowns are not particularly strong ligands for lithium amide monomers.[21b]

(28) (a) Romesberg, F. E.; Collum, D. B. *J. Am. Chem. Soc.* **1992**, *114*, 2112. (b) Bernstein, M. P.; Romesberg, F. E.; Fuller, D. J.; Harrison, A. T.; Williard, P. G.; Liu, Q. Y.; Collum, D. B. *J. Am. Chem. Soc.* **1992**, *114*, 5100. (c) Romesberg, F. E.; Bernstein, M. P.; Gilchrist, J. H.; Harrison, A. T.; Fuller, D. J.; Collum, D. B. *J. Am. Chem. Soc.* **1993**, *115*, 3475. (d) Romesberg, F. E.; Collum, D. B. *J. Am. Chem. Soc.* **1994**, *116*, 9187. (e) Romesberg, F. E.; Collum, D. B. *J. Am. Chem. Soc.* **1995**, *117*, 2166. (f) Koch, R.; Wiedel, B.; Anders, E. *J. Org. Chem.* **1996**, *61*, 2523. (g) McKee, M. L. *J. Am. Chem. Soc.* **1985**, *107*, 7284. (h) Viruela-Martin, P.; Viruela-Martin, R.; Tomás, F.; Nudelman, N. S. *J. Am. Chem. Soc.* **1994**, *116*, 10110. (i) Hilmersson, G.; Arvidsson, P. I.; Davidsson, O.; Håkansson, M. *J. Am. Chem. Soc.* **1998**, *120*, 8143. (j) Hilmersson, G.; Arvidsson, P. I.; Davidsson, O.; Håkansson, M. *Organometallics* **1997**, *16*, 3352.

(29) MNDO calculations exaggerate steric effects: Scano, P.; Thomson, C. *J. Comput. Chem.* **1991**, *12*, 172. Stewart, J. J. P. *J. Comput.-Aided Mol. Des.* **1990**, *4*, 1. Also, see ref 28a.

(30) (a) One could, at least in principle, separate effects due to ligand−ligand interactions from ligand−R_2NLi interactions by dissecting the solvation into two steps using the method reported by Hay and co-workers[30b] as follows: After location of the low-energy structures of η^1-solvated dimers and η^2-solvated dimers in Scheme 1, the Me_2NLi fragments were removed without modification of the chelating ligand. The strain energies of the resulting ligand conformers were obtained by a single-point calculation. Although this did not appear to offer compelling insights in this particular case, we have archived the results in Supporting Information. (b) Hay, B. P.; Rustad, J. R.; Hostetler, C. J. *J. Am. Chem. Soc.* **1993**, *11*, 5, 11158. Hay, B. P.; Rustad, J. R. *J. Am. Chem. Soc.* **1994**, *116*, 6316.

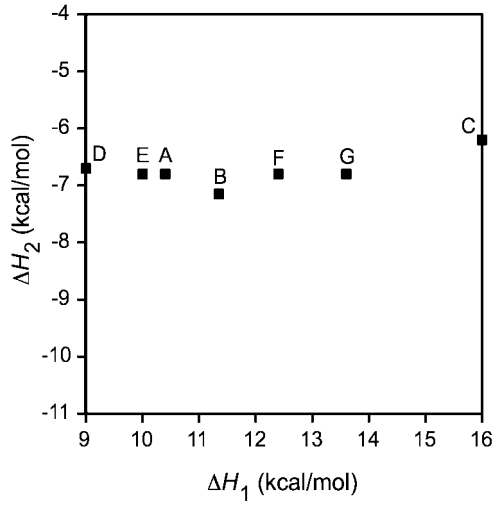

Figure 4. Plot of calculated ΔH_1 versus ΔH_2 (kcal/mol) for Me_2NLi coordinated to ligands of general structure $MeOCH_2CH_2NR_2$ (**A**−**G**).

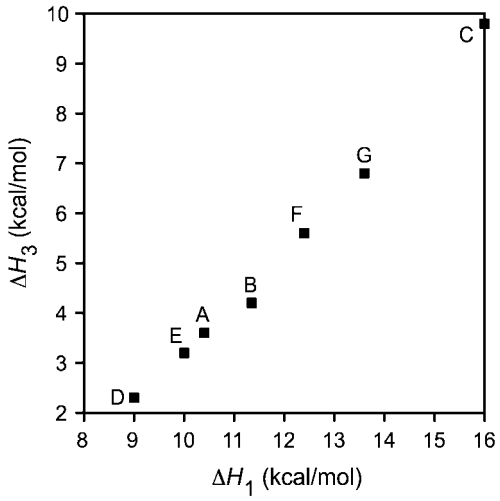

Figure 5. Plot of calculated ΔH_1 versus ΔH_3 (kcal/mol) for Me_2NLi coordinated to ligands of general structure $MeOCH_2CH_2NR_2$ (**A**−**G**).

ligand-dependent deaggregation for this structurally similar group of amino ethers is dictated almost entirely by ligand-dependent interactions within the chelated monomers. A comparison of the free energies of activation for the 1,2-elimination ($\Delta G^{\ddagger}_{rel}$) and the calculated enthalpies of deaggregation (ΔH_1) shows the over-estimation of steric effects by MNDO (Figure 6). The potentially aberrant results from aziridine-derived amino ether **D** may stem from the anomalously low basicities of aziridines.[31]

The amino ethers listed in Table 3 are characterized by substitution on the two-carbon backbone. The essence of a putative *gem*-dimethyl effect is that destabilizing intraligand and ligand−R_2NLi interactions in dimer **11** resulting from substitution within the ligand are alleviated on ring closure to form **12**. The effect is attenuated by substituent-derived ligand−R_2NLi and intraligand interactions within monomer **12**. A plot of ΔH_1 versus ΔH_2 (Figure 7) shows that deaggregation is indeed facilitated by poor coordination of ligand and dimer, as

(31) Searles, S.; Tamres, M.; Block, F.; Quaterman, L. A. *J. Am. Chem. Soc.* **1956**, *78*, 4917.

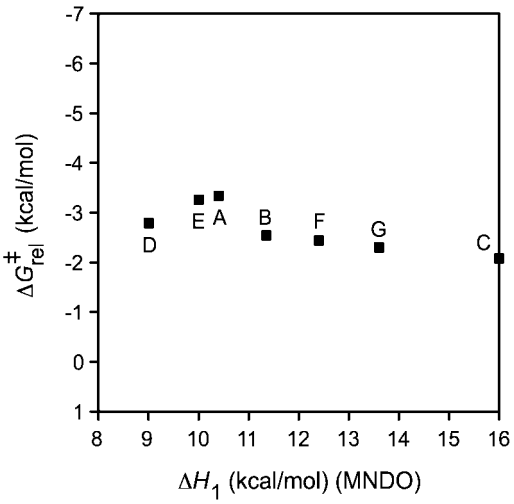

Figure 6. Plot of calculated ΔH_1 for Me_2NLi coordinated to ligands of general structure $MeOCH_2CH_2NR_2$ (**A**−**G**) versus free energies of activation $\Delta G^{\ddagger}_{rel}$ (kcal/mol) relative to *n*-BuOMe for the 1,2-elimination of 1-bromocyclooctene (**1**).

Table 3. Calculated Enthalpies (kcal/mol) of Monomer Aggregation (ΔH_1), Dimer Solvation (ΔH_2), and Monomer Solvation (ΔH_3) for Me_2NLi Coordinated to Ligands Substituted on the Two-Carbon Backbone[a]

ligand	$\Delta H_{f(Ligand)}$	ΔH_1	ΔH_2	ΔH_3
K	−35.0	8.7	−5.1	3.6
L	−38.9	8.2	−5.1	3.1
M	−43.3	9.1	−5.6	3.5
N	−46.9	8.2	−3.4	4.8
O	−44.2	8.5	−3.0	5.5
P	−44.4	8.5	−5.0	3.5
Q	−47.5	6.9	−3.0	3.9
R	−47.1	7.2	−2.1	5.1
S	−41.9	6.8	−2.7	4.1
T	−42.3	9.0	−4.0	5.0
U	−8.0	7.4	−3.3	4.1
V	−8.3	10.6	−5.9	5.5
av dev[b]	−	1.1	1.3	0.8

[a] The average deviation of the enthalpies is represented by. The heats of formation (kcal/mol) of ligands **K**−**V** in their most stable conformations is represented by $\Delta H_{f(Ligand)}$. $(Me_2NLi)_2 = -60.5$ kcal/mol. [b] Av dev = average deviation.

predicted. In contrast, a plot of ΔH_1 versus ΔH_3 (Figure 8) reveals a complex relationship between the enthalpy of aggregation and the enthalpy of monomer solvation. To some extent, the apparent scatter stems from the narrow range for ΔH_3. On closer inspection (Table 3), we cannot discern a relationship between ligand structure and deaggregation. Nevertheless, the substituent effects on the rate accelerations observed experimentally are muted compared with the analogous effects on the dimer−monomer deaggregations predicted computationally (Figure 9).

DFT Computational Studies. We addressed several lingering issues using DFT calculations performed at the B3LYP/6-31G* level of theory.[32,33] Me_2NLi and (*E*)-2-bromo-2-butene were

(32) Frisch, M. J.; Trucks, G. W.; Schlegel, H. B.; Scuseria, G. E.; Robb, M. A.; Cheeseman, J. R.; Zakrzewski, V. G.; Montgomery, J. A., Jr.; Stratmann, R. E.; Burant, J. C.; Dapprich, S.; Millam, J. M.; Daniels, A. D.; Kudin, K. N.; Strain, M. C.; Farkas, O.; Tomasi, J.; Barone, V.; Cossi, M.; Cammi, R.; Mennucci, B.; Pomelli, C.; Adamo, C.; Clifford, S.; Ochterski, J.; Petersson, G. A.; Ayala, P. Y.; Cui, Q.; Morokuma, K.; Malick, D. K.; Rabuck, A. D.; Raghavachari, K.; Foresman, J. B.; Cioslowski, J.; Ortiz, J. V.; Baboul, A. G.; Stefanov, B. B.; Liu, G.; Liashenko, A.; Piskorz, P.; Komaromi, I.; Gomperts, R.; Martin, R. L.; Fox, D. J.; Keith, T.; Al-Laham,

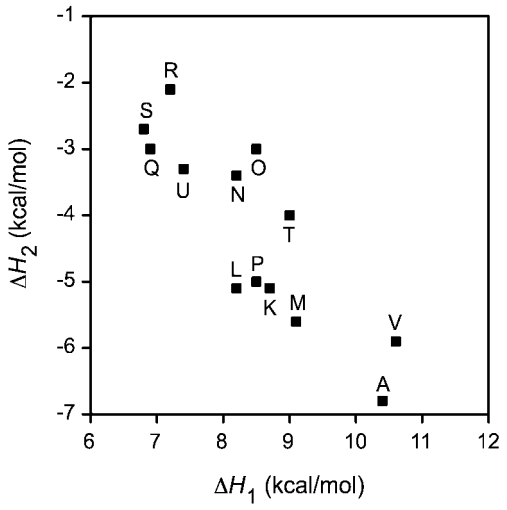

Figure 7. Plot of calculated ΔH_1 versus ΔH_2 (kcal/mol) for Me_2NLi coordinated to ligands substituted on the two-carbon backbone (**K**−**V**).

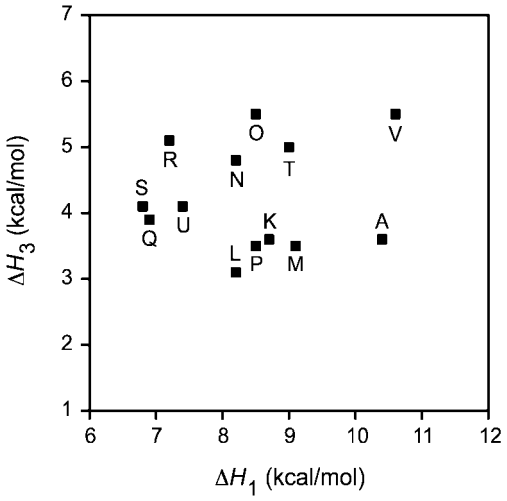

Figure 8. Plot of calculated ΔH_1 versus ΔH_3 (kcal/mol) for Me_2NLi coordinated to ligands substituted on the two-carbon backbone (**K**−**V**).

used as models for LDA and 1-bromocyclooctene, respectively. Substitution of *n*-BuOMe by DME or $MeOCH_2CH_2NMe_2$ in disolvated Me_2NLi dimers is calculated to be essentially thermoneutral; the calculated ligand-dependent activation energies ($\Delta E^{\ddagger}$) described below derive from differential stabilization of the transition structures. η^1-Bound ligand **A** is modeled using Me_2O to simplify the conformational effects. A range of initial geometries was sampled for all reactant and transition structures. Legitimate saddle points were shown by the existence of a single imaginary frequency.

Optimized transition structures **15**−**17** corresponding to $[(R_2NLi)(ligand)(RBr)]^{\ddagger}$ display nearly planar six-membered rings, essentially linear N−H−C angles,[34] and distinct Li−Br contacts independent of starting geometries (Chart 4, Table 4). Lengthening of the C−H and C−Br bonds in the transition structures compared with those in the starting vinyl bromide are consistent with concerted (E2-like) mechanisms.[35] The lengthening of the C−H bonds and shortening of the C−Br bonds coincide with decreasing $\Delta E^{\ddagger}$. The underestimated $\Delta E^{\ddagger}$ values are not uncommon.[36]

We begin by comparing $\Delta E^{\ddagger}$ values for the monomer solvated by Me_2O (**15**), η^2-**A** (**16**), and η^2-DME (**17**). In qualitative accord with experiment, the activation barriers via chelated transition structures are lower, although clearly the calculations overestimate the net stabilization. Moreover, chelated amino

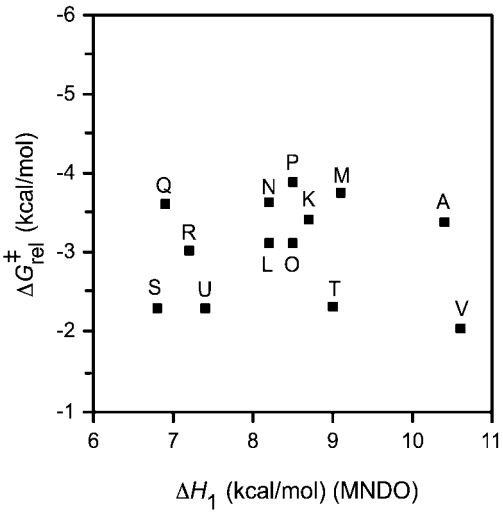

Figure 9. Plot of calculated ΔH_1 for Me_2NLi coordinated to ligands substituted on the two-carbon backbone (**K**-**V**) versus free energies of activation $\Delta G^{\ddagger}_{rel}$.

Chart 4. Calculated Activation Energies ($\Delta E^{\ddagger}$'s). the Energies Are Referenced to *E*-2-Bromo-2-butene and 1/2$(Me_2NLi)_2(\eta^1$-O-bound Ligand$)_2$

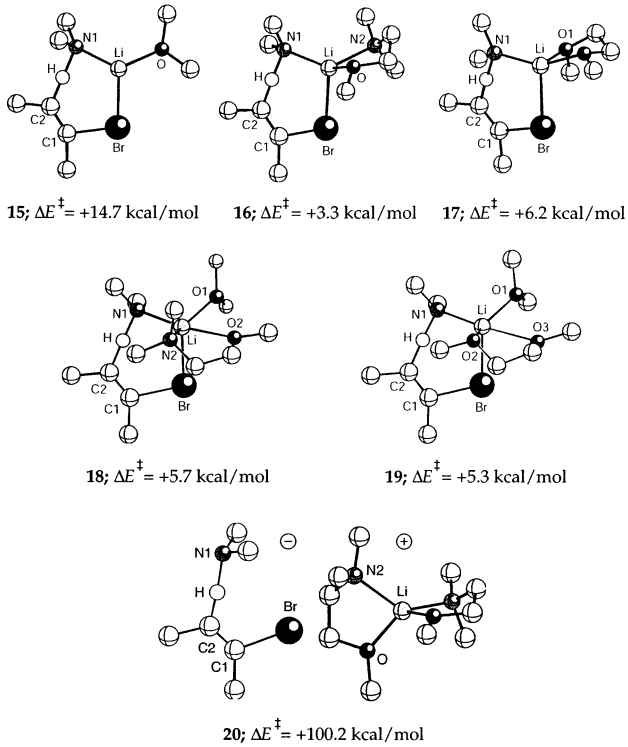

M. A.; Peng, C. Y.; Gill, A.; Nanayakkara, C.; Gonzalez, M.; Challacombe, P. M. W.; Johnson, B.; Chen, W.; Wong, M. W.; Andres, J. L.; Gonzalez, C.; Head-Gordon, M.; Replogle, E. S.; Pople, J. A. *Gaussian 98*; Gaussian, Inc.: Pittsburgh, PA, 1998.

(33) The Ahlrichs all-electron SVP basis set was used for Br, and 6-31G* was used for the rest. This basis set is denoted as 631A and has been previously applied to mechanistic studies on organolithium-mediated reactions: Nakamura, E.; Yamanaka, M.; Yoshikai, N.; Mori, S. *Angew. Chem., Int. Ed.* **2001**, *40*, 1935. Mori, J.; Nakamura, E.; Morokuma, K. *J. Am. Chem. Soc.* **2000**, *122*, 7294 and references therein.

(34) Narula, A. S. *Tetrahedron Lett.* **1981**, *27*, 4119.

Table 4. Selected Bond Lengths (Å) for Calculated Transition Structures **15**, **16**, **17**, **18**, **19**, and **20**

bond	15	16	17	18	19	20
Li−Br	2.38	2.48	2.49	2.56	2.55	−
Li−N(1)	1.92	1.94	1.93	2.03	2.03	−
Li−N(2)	−	2.15	−	2.40	−	2.12
Li−O(1)	1.92	2.02	2.05	2.22	2.13	1.98
Li−O(2)	−	−	2.04	2.38	2.24	−
Li−O(3)	−	−	−	−	2.52	−
Br−C(1)	2.31	2.21	2.22	2.18	2.17	2.05
C(1)−C(2)	1.28	1.29	1.29	1.30	1.30	1.31
C(2)−H	1.33	1.36	1.35	1.38	1.39	1.28
N(1)−H	1.39	1.36	1.38	1.34	1.33	1.47

ether (η^2-**A**) was predicted to be stabilizing when compared with η^2-DME, also in accord with experiment.

Recall that the least hindered amino ether **A** displayed a unique and previously unobserved tendency to promote reaction via a *disolvated* monomer−[(*i*-Pr_2NLi)(ligand)$_2$(**1**)]‡. We calculated that transition structures **18** and **19** bearing a five-coordinate lithium. The Li−Br linkage in **18** and **19** resides at the apex of a square pyramid (showing some distortion toward a trigonal bipyramid).[37] The stereoisomer of **18** bearing *trans*-disposed Me_2N moieties could not be found. DME solvate **19**, the structural analogue of **18**, could be found, albeit with a Li−O bond showing considerable lengthening.

The stabilizations of transition structures **18** and **19** by the η^1 ether linkage, although similar, appear to be opposite to the experimental observation. Whereas coordination of transition structure **16** by a molecule of Me_2O (a proxy for η^1-**A**) to form **18** is endothermic (+1.3 kcal/mol), the corresponding solvation of DME chelate **17** by Me_2O to form **19** is slightly exothermic (−0.8 kcal/mol). Thus, the calculations appear to predict that elimination via a more highly solvated transition structure was more likely in DME than in amino ether **A**.

The Li−Br linkage appears to be very important: All attempts to locate transition structures analogous to **8** and **9** missing the Li−Br linkage afforded structures with Li−Br contacts. Transition structure **20** (analogous to **10**), corresponding to a fully ionized lithium amide, receives very little support computationally, showing enormous destabilization. It seems unlikely that additional solvation of the lithium cation or inclusion of relatively small pairing energies[38] could compensate.

As an aside, the relative efficacies of amino ether **A** and DME (**CC**) to form high-coordinate lithium were evaluated using simple five-coordinate monomers **21** and **22** (Chart 5).[39] Both are found to be stable minima in trigonal bipyramidal geometries. (A minimum corresponding to the isomer of **21** manifesting an equatorial and apical Me_2N moiety was not found.) The methyl groups on the methoxy moieties of **22** reside proximate to the Me_2NLi fragment regardless of starting geometry. It is interesting that the minimized structures for **21** and **22** are quite similar to the crystal structures of $LiBF_4$(**A**)$_2$ (**23**) and $LiBF_4$(DME)$_2$ (**24**), also illustrated in Chart 5.[40] The relative propensities of amino ether **A** and DME to support high coordination are shown by the exothermic substitution of DME by amino ether **A** (−1.1 kcal/mol).[41]

Chart 5. Comparison of X-ray Crystal Structures for Bis-chelated $LiBF_4$ (**23** and **24**) with Bis-chelated Me_2NLi Calculated with DFT (**21** and **22**)

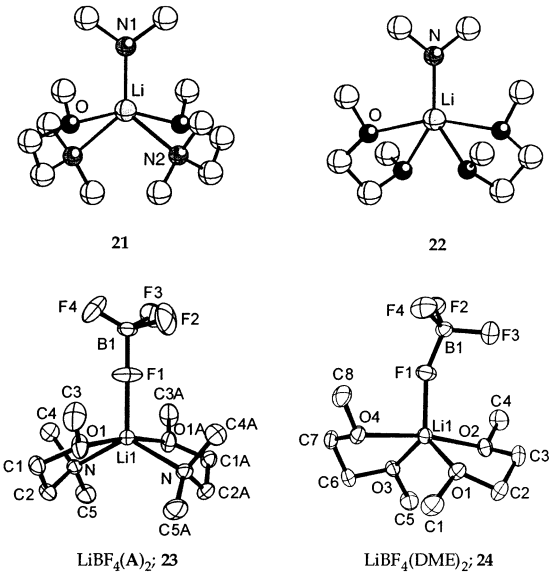

Discussion

We have used LDA solvated by hemilabile amino ethers and diethers to determine whether the *gem*-dimethyl effect influences the stabilities of chelates relative to their nonchelated counterparts. These studies underscore the complexities of metal−ligand interactions and the challenges affiliated with addressing the key questions. Before we can consider the factors that influence stabilities of chelates and how chelate stabilities influence reaction rates, we must establish a firm understanding of some general issues.

Structure and Mechanism. Spectroscopic, kinetic, and computational methods are highly synergistic. Structural studies show that LDA solvated by a range of aminoethers and diethers yields *O*-bound dimers of general structure **3**. The well-documented low affinities of the dialkylamino groups for lithium amide dimers,[1,21] although counterintuitive on the basis of

(35) Considerable evidence points to a continuum of mechanisms in the range E2−E1cb for the elimination of HX from halo-substituted alkenes: Komatsu, K.; Aonuma, S.; Jinbu, Y.; Tsuji, R.; Hirosawa, C.; Takeuchi, K. *J. Org. Chem.* **1991**, *56*, 195. Shahlai, K.; Hart, H. *J. Am. Chem. Soc.* **1988**, *110*, 7136. Bach, R. D.; Evans, J. C. *J. Am. Chem. Soc.* **1986**, *108*, 1374. Gassman, P. G.; Gennick, I. *J. Am. Chem. Soc.* **1980**, *102*, 6863. Gassman, P. G.; Valcho, J. J. *J. Am. Chem. Soc.* **1975**, *97*, 4768. Modena, G.; Marchese, G.; Naso, F.; Tangari, N. *J. Chem. Soc. B* **1970**, 1196. Kwok, W. K.; Lee, W. G.; Miller, S. I. *J. Am. Chem. Soc.* **1969**, *91*, 468. Marchese, G.; Modena, G.; Naso, F. *J. Chem. Soc. B* **1968**, 958. Miller, S. I.; Lee, W. G. *J. Am. Chem. Soc.* **1959**, *81*, 6313.

(36) Haffner, F.; Sun, C.; Williard, P. G. *J. Am. Chem. Soc.* **2000**, *122*, 12542.

(37) For examples of trigonal bipyramidal pentacoordinated lithium amide monomers, see: Poetschke, N.; Nieger, M.; Khan, M. A.; Niecke, E.; Ashby, M. T. *Inorg. Chem.* **1997**, *36*, 4087. Kremer, T.; Hampel, F.; Knoch, F. A.; Bauer, W.; Schmidt, A.; Gabold, P.; Schtz, M.; Ellermann, J.; Schleyer, P. v. R. *Organometallics* **1996**, *15*, 4776.

(38) Yakimansky, A. V.; Müller, A. H. E. *J. Am. Chem. Soc.* **2001**, *123*, 4932. Badiali, J.-P.; Cachet, H.; Cyrot, A,; Lestrade, J.-C. *J. Chem. Soc., Faraday Trans.* **1973**, 1339. Cachet, H.; Cyrot, A.; Fekir, M.; Lestrade, J.-C. *J. Phys. Chem.* **1979**, *83*, 2419. Ashby, E. C.; Dobbs, F. R.; Hopkins, H. P., Jr. *J. Am. Chem. Soc.* **1973**, *95*, 2823. Matsuda, Y.; Morita, M.; Tachihara, F. *Bull. Chem. Soc. Jpn.* **1986**, *59*, 1967. Delsignore, M.; Maaser, H. E.; Petrucci, S. *J. Phys. Chem.* **1984**, *88*, 2405. Tobishima, S.; Yamaji, A. *Electrochim. Acta* **1983**, *28*, 1067. See also refs 38a, c−e.

(39) Evidence of high-coordinate lithium amides: (a) Lucht, B. L.; Collum, D. B. *J. Am. Chem. Soc.* **1995**, *117*, 9863. (b) Lucht, B. L.; Bernstein, M. P.; Remenar, J. F.; Collum, D. B. *J. Am. Chem. Soc.* **1996**, *118*, 10707. (c) Depue, J. S.; Collum, D. B. *J. Am. Chem. Soc.* **1988**, *110*, 5524. (d) Henderson, K. W.; Dorigo, A. E.; Liu, Q.-Y.; Williard, P. G. *J. Am. Chem. Soc.* **1997**, *119*, 11855. (e) See ref 37.

(40) The key structural data for the crystal structures **23** and **24** are located in Supporting Information and have been archived in the Cambridge Crystallographic Database (**23**, CCDC 208621; **24**, CCDC 208620).

(41) March, J. *Advanced Organic Chemistry*; Wiley: New York, 1992, Chapter 8. Gutmann, V. *The Donor-Acceptor Approach to Molecular Interactions*; Plenum: New York, 1978. Marcus, Y. *J. Solution Chem.* **1984**, *13*, 599.

standard Lewis acid−base studies,[41] stem from the high steric demands of both the amino group and the lithium amide. Rate studies showed that the LDA-mediated dehydrohalogenations (eq 1), in the presence of a selected group of ligands (Table 1), all proceed via monomer-based mechanisms described generically in eqs 4−6. (A single exception is discussed below.)

Reference State. Any question pertaining to relative stability must confront the problem of choosing a reference state: Chelates may be stable, but relative to what?[15] This contribution is emblematic of the problem even in its simplest form in that we have alluded to *three* reference states to describe chelate stabilities.

(1) Relative chelate stabilities can be determined from relative binding constants starting with either a monomer (eq 10) or a dimer (eq 11). Although the absolute binding constants depend on whether the monomer or dimer is used, the *relative* binding constants will not change. (Two lithium amides differing in their *N*-alkyl groups, however, will afford different *relative* binding constants.) In this case, the relative stabilities of the chelates are referenced to the free ligands. This method was used computationally in Scheme 2 (ΔH_3). On several occasions, it has also been used in conjunction with NMR spectroscopy to measure relative binding constants of chelating ligands to lithium amides.[42,43]

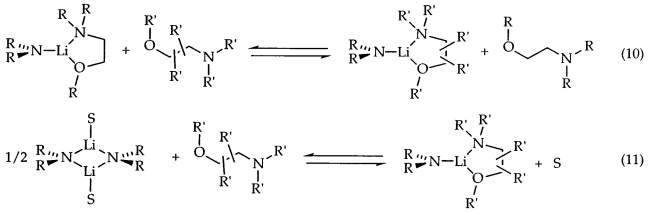

(10)

(11)

(2) The ligand-dependent stabilities of the chelates can be compared to the ligands bound in the η^1-solvated dimers (eq 12) rather than in the free ligands. To the extent that the η^1-coordinated ligands are in highly constrained environments within the dimer, potentially significant *i*-Pr_2NLi−ligand and intraligand interactions in the dimer and monomer will influence the *relative* stabilities of the chelated monomer. This approach is used to calculate ΔH_1 in Scheme 2. Importantly, referencing the chelate stabilities to the free ligands as in eq 10 or 11 or to the η^1 ligands as in eq 12 will *not* necessarily provide even the same *relative* binding constants. Indeed, the calculated values of ΔH_1 and ΔH_3 display only a modest correlation (Figure 8).

(3) The ligand-dependent activation energies for the elimination of the vinyl halide (eq 13) are also referenced to η^1-solvated dimers. The existence of the vinyl bromide fragment in the transition structures, however, introduces unique interactions with the substrate as well as altered intraligand and R_2NLi−ligand interactions in the chelate. Consequently, although the methods delineated in eqs 12 and 13 bear similarities, the two methods are not directly comparable. Relative binding affinities of ligands to the monomeric transition structure—[(R_2NLi)(ligand)(RBr)]‡—and a simple monomer—(R_2NLi)(ligand)—will

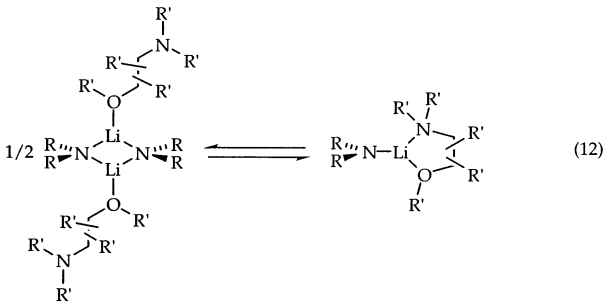

(12)

not correlate unless the environments within the coordination spheres of the two forms are markedly similar.

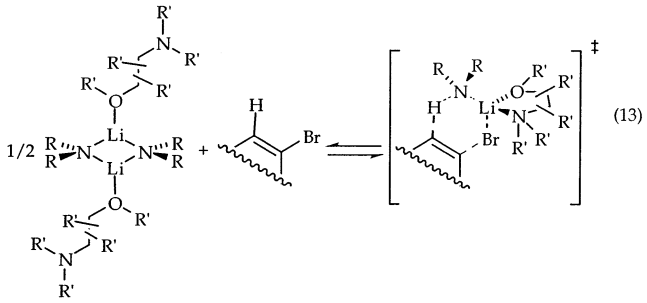

(13)

The three means of measuring ligand binding share a common theme: They probe the ligand-dependent stabilities of chelates. The reference-state-dependent *relative* binding constants may be somewhat unsettling, but it is unavoidable. In the sections that follow, we discuss factors influencing ligand-dependent binding and affiliated reaction rates. Although our interests are largely in the experimental arena, the computational results summarized in Scheme 2 are pedagogically useful.

Hemilability. It is instructive to consider first the basic principles of hemilability as illustrated structurally in Scheme 1 and thermochemically in Figure 10. Previous experimental studies had shown that unsubstituted amino ethers ($MeOCH_2CH_2NR_2$), unsubstituted diethers ($MeOCH_2CH_2OR$), and *n*-BuOMe bind to LDA dimers (**3**) with equal affinities—$\Delta G°_{GS} = 0$ (Figure 10).[1] The relative rate constants for the eliminations by the amino ethers and diethers provide a direct measure of relative stabilizations attributed to chelation at the transition state, $\Delta G°_{TS}$. Indeed, we found that simple vicinal diethers and amino ethers afford large (up to 10^3-fold) accelerations when compared with *n*-BuOMe (Chart 1). The maximal acceleration (reflected by a large ΔG_{TS}) for the simple bifunctional ligands ($MeOCH_2CH_2L$) is observed for the sterically least demanding amino ether **A**.

We probed hemilability with semiempirical computational studies using Me_2NLi as a model for LDA and *n*-BuOMe. The ligand-dependent transition structures using (*E*)-2-bromo-2-butene as the substrate proved too congested for the sterically sensitive semiempirical methods. Consequently, we surveyed the ligand-dependent deaggregation in Scheme 2. The calculations confirm the equivalent binding constants for a range of ligands of general structure $MeOCH_2CH_2L$ (Scheme 1, ΔH_2). (Limited DFT studies concurred.) The aggregation enthalpy (ΔH_1) is dictated almost entirely by the relative solvation enthalpies of the monomer (ΔH_3), as illustrated Figures 4 and 5. This result is qualitatively consistent with the notion that the ligand-dependent rates for the structurally simple ligands,

(42) Remenar, J. F.; Lucht, B. L.; Kruglyak, D.; Romesberg, F. E.; Gilchrist, J. H.; Collum, D. B. *J. Org. Chem.* **1997**, *62*, 5748. Hoffmann, D.; Collum, D. B. *J. Am. Chem. Soc.* **1998**, *120*, 5810. See refs 18a and 39.

(43) Emmenegger, F.; Schlaepfer, C. W.; Stoeckli-Evans, H.; Piccand, M.; Piekarski, H. *Inorg. Chem.* **2001**, *40*, 3884. Smith, D. C.; Haar, C. M., Jr.; Stevens, E. D.; Nolan, S. P. *Organometallics* **2000**, *19*, 1427. Hancock, R. D. *J. Chem. Educ.* **1992**, *69*, 615. See also ref 3.

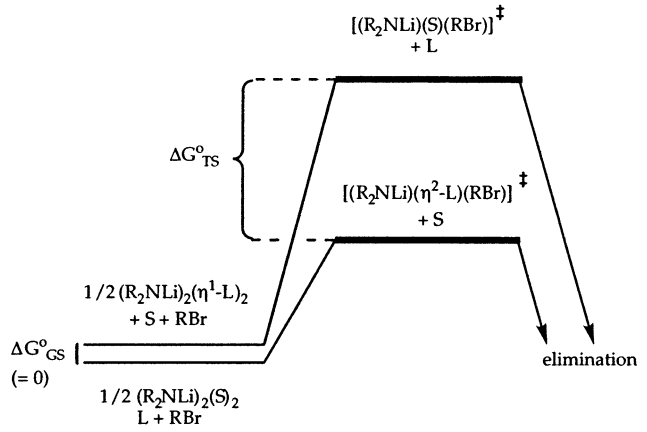

Figure 10.

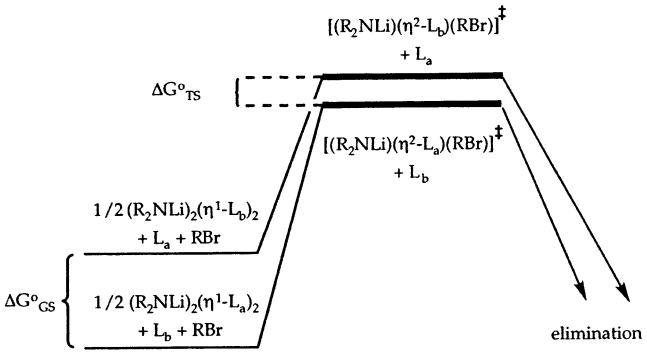

Figure 11.

$MeOCH_2CH_2L$, derive from the exclusively differential stabilities of the chelated transition structures. Moreover, the results highlight the utility of hemilabile ligands as diagnostic probes of chelate stability.

***gem*-Dimethyl Effect.** We are now poised to address the question: Is there a *gem*-dimethyl effect on lithium ion chelation? In a more general sense, do substituents along the ligand backbone promote chelation? Once again, it is instructive to describe the *gem*-dimethyl effect in the context of a simple thermochemical picture (Figure 11). In the *gem*-dimethyl effect, destabilizing interactions in the acyclic reactant (reflected by a ligand-dependence of ΔG_{GS}) are attenuated or alleviated in the cyclic transition structure (reflected in ΔG_{TS}), resulting in promotion of the cyclic form—$\Delta G_{TS} \ll \Delta G_{GS}$. The effect will be diminished if these interactions are incompletely alleviated at the transition structure or if there are destabilizing interactions unique to the transition structure.

Inspection of the relative rate data listed in Chart 2 suggest that *the gem-dimethyl effect is of little consequence*. Although amino ethers bearing a single, sterically undemanding substituent along the ligand backbone—ligands **M**, **N**, **P**, and **Q**—measurably increased the rates of elimination, the accelerations are miniscule compared with the 10^4-fold accelerations noted in some cyclization reactions.[8,14] Highly substituted ligands, including geminally dimethylated amino ethers **K** and **L**, afford muted rates compared to **A**. A more randomly chosen group of ligands (Chart 3) uncovered no special accelerations either.

It seems appropriate to rephrase the title question: Why is there no *gem*-dimethyl effect on lithium ion chelation? Although this is an exceedingly challenging question, we can at least attempt to bring the key issues into focus. Curiously, even investigations of chelation in transition metal chemistry are surprisingly nonsystematic, offering little assistance in sorting through many of the factors influencing chelation of lithium.[44,45] It might be tempting to take a traditional approach by dissecting the rates into enthalpic and entropic effects.[46] Unfortunately, steric effects are the dominant contribution to the energy of lithium−ligand interactions,[21b,39] and they have both enthalpic and entropic components.[47,48] It is not obvious to us that such a dissection affords special insights. Instead, we choose to simply discuss the factors influencing the relative stabilities of the η^1-solvated dimers and η^2-solvated monomers. It is important to recognize that a discussion of highly interdependent variables as separate contributions is artificial.

(1) Buttressing. We believe that conformational buttressing may be the most dominant contribution to destabilization of the chelates. It is well documented that dimeric lithium amides are very sensitive to the steric demands of solvation.[28] In principle, severe buttressing will exacerbate these interactions, leading to a net *relative* stabilization of chelated forms. In practice, however, the *contiguous functionalized atoms* in the chelates may also suffer from severe buttressing, in turn, eliminating the elusive *gem*-dimethyl effect.

(2) Ring size. Previous studies have shown that five-membered chelates are much more stable than their four- and six-membered counterparts for a range of chelating amino ethers, diethers, and diamines coordinated to lithium amides.[49,50] Reich has observed similar trends in organolithiums bearing an internal

(44) Breslow, R.; Belvedere, S.; Gershell, L.; Leung, D. *Pure Appl. Chem.* **2000**, *72*, 333. van Leeuwen, P. W. N. M.; Kamer, P. C. J.; Reek, J. N. H.; Dierkes, P. *Chem. Rev.* **2000**, *100*, 2741. Busch, D. H. *Chem. Rev.* **1993**, *93*, 847. Hancock, R. D.; Martell, A. E. *Chem. Rev.* **1989**, *89*, 1875. Cotton, F. A.; Wilkinson, G. *Advanced Inorganic Chemistry* 5th ed.; Wiley: New York; 1988; pp 45−48. Huheey, J. E. *Inorganic Chemistry: Principles of Structure and Reactivity* 3rd ed.; Harper and Row: Cambridge, 1983. Butler, I. S.; Harrod, J. F. *Inorganic Chemistry: Principles and Applications*; Bejamin/Cummings: Redwood City, 1989; p 366. Wulfsberg, G. *Principles of Descriptive Inorganic Chemistry*; Brooks/Cole: Monterey, CA, 1987; pp 247−248.

(45) Ligand parameters have been developed to understand chelating ligands in transition metal chemistry: (a) Bite angle: Casey, C. P.; Paulsen, E. L.; Beuttenmueller, E. W.; Proft, B. R.; Petrovich, L. M.; Matter, B. A.; Powell, D. R. *J. Am. Chem. Soc.* **1997**, *119*, 11817. (b) Pocket angle: Koide, Y.; Bott, S. G.; Barron, A. R. *Organometallics* **1996**, *15*, 2213. (c) Accessible molecular surface: Angermund, K.; Baumann, W.; Dinjus, E.; Fornika, R.; Görls, H.; Kessler, M.; Krüger, C.; Leitner, W.; Lutz, F. *Chem. Eur. J.* **1997**, *3*, 755.

(46) Minahan, D. M. A.; Hill, W. E.; McAuliffe, C. A. *Coord. Chem. Rev.* **1984**, *55*, 31. Chung, C.-S. *J. Chem. Educ.* **1984**, *61*, 1062. Myers, R. T. *Inorg. Chem.* **1978**, *17*, 952. Smith, R. M.; Martell, A. E. *Critical Stability Constants*; Plenum Press: New York, 1975; Vol. 2. See also refs 3b and 4.

(47) Westheimer, F. H. In *Steric Effects in Organic Chemistry*; Newman, M. S. Ed.; Wiley: New York, 1956.

(48) Manifestation of a steric effect as an entropic contribution has been referred to as population control. Winans, R. E.; Wilcox, C. F., Jr. *J. Am. Chem. Soc.* **1976**, *98*, 4281. For entropically dominated solvent-dependent ion pairing that may be related, see: Strong, J.; Tuttle, T. R., Jr. *J. Phys. Chem.* **1973**, *77*, 533.

(49) Reich, H. J.; Kulicke, K. J. *J. Am. Chem. Soc.* **1996**, *118*, 273. Reich, H. J.; Kulicke, K. J. *J. Am. Chem. Soc.* **1995**, *117*, 6621. Morton, M. D.; Heppert, J. A.; Dietz, S. D.; Huang, W. H.; Ellis, D. A.; Grant, T. A.; Eilerts, N. W.; Barnes, D. L.; Takusagawa, F.; VanderVelde, D. *J. Am. Chem. Soc.* **1993**, *115*, 7916. Hancock, R. D. *Acc. Chem. Res.* **1990**, *23*, 253. Hancock, R. D.; Ngwenya, M. P. *J. Chem. Soc., Dalton Trans.* **1987**, 2911. Barbucci, R.; Fabbrizzi, L.; Paoletti, P. *Inorg. Chim. Acta* **1973**, *7*, 157. Gillard, R. D.; Irving, H. M. *Chem. Rev.* **1965**, *65*, 603.

(50) Stabilization of five-membered chelates for a number of metals has been attributed to an enthalpy effect associated with greater distortion induced in the complex upon closure for a six-membered ring: Munakata, M.; Kitagawa, S.; Yagi, F. *Inorg. Chem.* **1986**, *25*, 964. Dobson, G. R.; Dobson, C. B.; Mansour, S. E. *Inorg. Chem.* **1985**, *24*, 2179. Bisi-Castellani, C.; Maresca, L.; Natile, G. *Inorg. Chim. Acta* **1984**, *89*, 157. Tobe, M. L.; Schwab, A. P.; Romeo, R. *Inorg. Chem.* **1982**, *21*, 1185. Reisner, G. M.; Bernal, I.; Dobson, G. R. *J. Organomet. Chem.* **1978**, *157*, 23. Knebel, W. J.; Angelici, R. J. *Inorg. Chem.* **1974**, *13*, 627. Dudev, T.; Lim, C. *J. Am. Chem. Soc.* **1998**, *120*, 4450.

coordinating ligand.[51] Therefore, the role of ring size was not a major focus in this study. MNDO computational studies (archived in Supporting Information) confirm that the six-membered chelates are destabilized. That is not to say, however, that we understand *why* five is such a strongly preferred ring size.

(3) Aza- versus oxaphilicity. We have compared both oxygen- and nitrogen-based pendant ligands and have found on a number of occasions that monomers show a marked azaphilicity, whereas lithium amide dimers do not.[1,21b] Part of the increased azaphilicity of monomers relative to dimers is steric: The monomers are more accessible to the congested trialkylamines. The relative azaphilicity appears to increase with increasing Lewis acidity of the lithium cation.[52] The net effect is that hemilabile amino ethers routinely impart higher accelerations and promote deaggregations much more effectively than do their diether counterparts. This observation is in reasonable accord with the results of the DFT calculations (cf. **16** and **17** and Chart 4).

(4) R_2N moiety. As discussed above, the relative stabilities of the dimer−monomer equilibria (Scheme 2) and the relative activation energies (Chart 1) show that larger R_2N groups destabilize the chelated forms, presumably due to congestion within the lithium coordination sphere. This destabilization is reflected by a modest correlation of the experimental relative activation energies ($\Delta G^{\ddagger}_{rel}$) with the enthalpies of aggregation (ΔH_1, Scheme 2) shown in Figure 6. The scatter seen in Figure 6 may stem in part from a somewhat nonoptimal comparison of experimental results for LDA and computational results from Me_2NLi.

(5) RO moiety. Compelling experimental and computational evidence suggests that increasing steric demands of the coordinated alkoxy group of the η^1-solvated dimers (**3**) will introduce destabilizing steric effects.[39a] To the extent that a monomeric transition structure (**5**) *could* be considerably less sterically demanding, large accelerations might arise due to steric relief independent of chelation.[53] The MNDO computational studies on the model system in Scheme 2 suggest that increasing steric demands of ligands **H**, **I**, and **J** will promote formation of the monomer **12** (eq 12). Nonetheless, the experimental results using those same ligands show that the elimination rates *decrease* with increasing steric demand of the alkoxy moiety (cf. **A** and **H**−**J** and Chart 1). Therefore, there may be a considerably greater congestion in the monomer-based transition structures than in the simple monomers (cf., **25** and **26**).[54] This result is not surprising.

(6) Backbone substitution. On first inspection, substitution along the ligand backbone would seem to cause potentially severe intraligand and ligand−R_2N interactions in the dimers (**11**), in turn promoting monomers formation (**12**). However, it is difficult to assess the analogous interactions arising in the monomers. Indeed, both experimental and computational evidence indicate that the steric-induced deaggregation is both

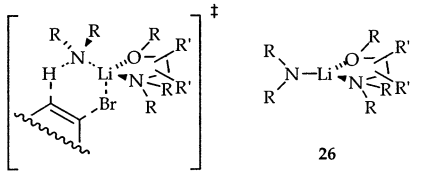

25 **26**

muted and complex, suggesting either that the interactions within the dimer are limited or that the interactions within the monomers are substantial. As noted in part 3, the monomer-based transition structures are highly sensitive to steric effects. Using a simple analogy with cyclopentanes,[55] one might have predicted that stereochemical effects in cis-trans pairs **S**/**T** or **U**/**V** would be pronounced, yet the differences are small. Overall, although there are instances in which deaggregation is promoted by bulk along the ligand backbone, once again the evidence indicates that substitution tends to destabilize the monomer-based transition structures relative to the disolvated dimers.

Elimination Via High-Coordinate LDA. Investigations of the elimination mediated by LDA/**A** mixtures revealed a solvent-dependent term in the rate law that had not appeared in previous studies. Distinguishing primary shell solvation from secondary shell can be challenging. Secondary shell solvation effects—so-called medium effects—on the chemistry of lithium amides have been observed, but they seem to be the exception rather than the rule.[26] These secondary shell effects are characterized by an insensitivity to substituents. This particular dependence on the concentration of amino ether **A**, however, was very sterically sensitive, offering compelling evidence of a primary shell solvation. Highly solvated transition structures **6**−**10** were modeled using DFT methods at the B3LYP/6-31G* level of theory using Me_2NLi, as illustrated in Chart 4. In short, transition structure **16** bearing a distinct Li−Br interaction is strongly preferred. The ionized form **19** is particularly unfavorable. The calculations suggest that DME promotes a high-coordinate lithium when compared with the amino ether **A**, whereas experiments indicate the contrary.[56] Overall, such high-coordinate lithium amides seem somewhat counterintuitive when considered in the context of steric demands, yet evidence of their existence and importance keeps surfacing.[39]

Summary and Conclusion

It is unclear at this time whether the *gem*-dimethyl effect is inconsequential in all of coordination chemistry, but it certainly failed to appear in the study described herein. Given the potential practical applications of understanding how ligand structures influence relative chelate stabilities, we find that discussions of chelation that focus on bite angles or that simply dissect free energies into enthalpies and entropies seem to ignore the key van der Waals interactions within the nonchelated and chelated forms. It seems likely that progress toward a thorough understanding of the chelate effect will depend on software and hardware developments supporting computational chemistry. We

(51) Reich, H. J.; Goldenberg, W. S.; Sanders, A. W.; Tzschucke, C. C. *Org. Lett.* **2001**, *3*, 33 and ref 3a.
(52) Salai Cheettu Ammal, S.; Venuvanalingam, P. *J. Chem. Soc., Faraday Trans.* **1998**, 2669. Yamamoto, H. In *Lewis Acids in Organic Synthesis*; Saito, S., Ed.; VCH: Weinheim, 2000; Chapter 1, p 9.
(53) Zhao, P.; Collum, D. B. *J. Am. Chem. Soc.* **2003**, *125*, 4008. Zhao, P.; Collum, D. B. *J. Am. Chem. Soc.* **2003**, *125*, 14411.
(54) LDA/*t*-BuOMe shows a 1.5-fold acceleration when compared with LDA/*n*-BuOMe.
(55) (a) Christl, M.; Reich, H. J.; Roberts, J. D. *J. Am. Chem. Soc.* **1971**, *93*, 3463. Allinger, N. L.; Hirsch, J. A.; Miller, M. A.; Tyminski, I. J.; VanCatledge, F. A. *J. Am. Chem. Soc.* **1968**, *90*, 1199. (b) Trans substituents are suggested to be preferred in transition metal chelates: Brubaker, G. R.; Johnson, D. W. *Coord. Chem. Rev.* **1984**, *53*, 1.
(56) Promotion of higher solvation by coordinated amines has been noted. Reich, H. J.; Goldenberg, W. S.; Gudmundsson, B. Ö.; Sanders, A. W.; Kulicke, K. J.; Simon, K.; Guzei, I. *J. Am. Chem. Soc.* **2001**, *123*, 8067.

do believe, however, that progress can be made through experimental studies of structure-dependent binding constants and correlations of binding constants with reactivity.

Experimental Section

Reagents and Solvents. Ligands **CC**−**GG**, **JJ**, **KK**, **MM**−**QQ** were obtained from commercial sources. Ligands **A**−**J**, **L**, **M**, **P**, **S**−**Z**, and **AA** were prepared following described procedures.[18] Details for the preparation and characterization of ligands **K**, **N**, **O**, **Q**, **R**, **BB**, and **LL** are available in Supporting Information. All solvents were distilled by vacuum transfer from sodium benzophenone ketyl. The hydrocarbon stills contained 1% tetraglyme to dissolve the ketyl. 1-Bromocyclooctene (**1**) and the deuterated derivative were prepared according to literature methods.[25] The LDA was prepared as a solid with commercial *n*-BuLi and purified by the standard literature procedure.[17] The diphenylacetic acid used to check solution titers[57] was recrystallized from methanol and sublimed at 120 °C under full vacuum. Air- and moisture-sensitive materials were manipulated under argon or nitrogen following standard glovebox, vacuum line, and syringe techniques.

Kinetics. The rate studies were carried out as described previously[1] and are described in detail in the Supporting Information.

MNDO Computational Studies. MNDO calculations[28] were performed using the MOPAC[58] program with lithium parameters generated by Clark and Thiel.[59] All structures were fully optimized under the more rigorous criteria of the keyword PRECISE with no constraints. Each reported heat of formation ($\Delta H°$) is the result of a search for the global minimum starting from several different initial geometries. Symmetrical structures were reoptimized from distorted geometries to ensure that the symmetry is not an artifact. For more sterically crowded systems, the keyword GEO-OK was used with caution to override the small interatomic distance check.

Acknowledgment. We thank the National Institutes of Health for direct support of this work as well as Dupont Pharmaceuticals (Bristol-Myers Squibb), Merck Research Laboratories, Pfizer, Aventis, R.W. Johnson, Boehringer-Ingelheim, and Schering Plough for indirect support. We also acknowledge the National Science Foundation Instrumentation Program (CHE 7904825 and PCM 8018643), the National Institutes of Health (RR02002), and IBM for support of the Cornell Nuclear Magnetic Resonance Facility.

Supporting Information Available: Tabular and graphical presentation of rate data as well as general experimental methods (PDF). X-ray crystallographic file in CIF format. This material is available free of charge via the Internet at http://pubs.acs.org.

JA030322D

(57) Kofron, W. G.; Baclawski, L. M. *J. Org. Chem.* **1976**, *41*, 1879.
(58) Dewar, M. J. S.: Thiel, W. *J. Am. Chem. Soc.* **1977**, *99*, 4899.
(59) Thiel, W.; Clark, T. Unpublished results.